Journal Name

ARTICLE

Messenger RNA delivery by hydrazone-activated polymers

Marisa Juanes,[a] Oliver Creese,[b] Francisco Fernandez-Trillo[b,*] and Javier Montenegro[a,*]

Received 00th January 20xx,
Accepted 00th January 20xx

DOI: 10.1039/x0xx00000x

www.rsc.org/

The intracellular delivery of DNA and RNA therapeutics requires the assistance of vectors and/or nucleotide modifications to protect the nucleic acids against host nucleases and promote cellular internalization and release. Recently, messenger RNA (mRNA) has attracted much attention due to its transient activity and lack of genome permanent recombination and persistent expression. Therefore, there is a strong interest in the development of conceptually new non-viral vectors with low toxicity that could improve mRNA transfection efficiency. We have recently introduced the potential of polyhydrazones and the importance of the polymerization degree for the delivery of siRNA and plasmid DNA. Here, we demonstrate that this technology can be easily adapted to the more interesting complexation and delivery inside living cells cells of messenger RNA. The polyplexes resulting from the combination of the amphiphilic polyhydrazone were characterized and the transfection efficiency and cell viability were studied for a discrete collection of functionalized polyhydrazones. The results obtained demonstrated the versatility of these polymeric vectors as excellent candidates for the delivery of messenger RNA and validate the easy adaptability of the technology to more sensitive and therapeutically relevant nucleic acids.

1. Introduction

The delivery of nucleic acids (DNA or RNA) as therapeutic agents has focused the interest of chemists, pharmacists and materials scientists.[1] Therapeutic nucleic acids have been used to regulate gene expression as a treatment for heritable and acquired diseases, including the use of DNA-based vaccines, antiviral therapies or cancer immunotherapy.[2–4] Several reports highlight the great potential of messenger RNA (mRNA) in chemical biology and for the treatment of different diseases.[5–11] mRNA has an ideal transitory activity and it does not need to cross the nuclear envelope.[12] These intriguing properties have fuelled the search of messenger RNA therapies and for instance, mRNA has been successfully used in clinical trials such as cancer immunotherapy,[13] the treatment of infectious diseases[14] and in regenerative medicine.[15] Different from small interfering RNA (siRNA), the therapeutic use of mRNA is based on the potential to introduce new genetic information for the expression of therapeutic or essential proteins. However, mRNA has important advantages over the delivery of plasmid DNA (pDNA). mRNA target is located in the cytosol of the cell, whereas pDNA functionality requires reaching the nuclei and can be dependent on nuclear membrane breakdown during cell division.[12] Moreover, the risk of insertional mutagenesis, associated to pDNA, can be excluded when using mRNA.[16,5] However, the clinical translation of mRNA therapy is severely limited by the lack of stable and effective delivery vehicles.

The use of viruses as vectors for gene delivery comprises the majority of the current literature on this topic, as could be expected from their higher *in vivo* transfection efficiency.[17] However, the biological application of viral vectors has important limitations such as low DNA packaging capacity, insertional mutagenesis, undesirable immune responses and the critical problem of synthetic scaling up and production in large quantities.[17] Non-viral vectors, such as peptides,[18–21] lipid nanoparticles[22–24] and polymers,[25–28] have been intensively investigated for nucleic acid delivery as a safer, more reproducible and inexpensive alternative. The importance of non-viral vectors is highlighted by the recent approval of patisiran, a lipidic formulation of siRNA, for the treatment of Hereditary Transthyretin Amyloidosis.[29]

Supramolecular chemistry[30] has also been explored and applied in the search of conceptually new non-viral vectors based in lipids,[31] cyclodextrins,[32] pillararenes,[33] proteins,[34,35] peptides,[36,37] nanotubes[38] and other architectures.[39,40] Dynamic covalent chemistry has also recently emerged as a promising tool for delivery applications including nucleic acids.[41,42] Among all these

[a] Centro Singular de Investigación en Química Biolóxica e Materiais Moleculares (CIQUS), Departamento de QuímicaOrgánica, Universidade de Santiago de Compostela, 15782 Santiago de Compostela, Spain,
e-mail: Javier.montenegro@usc.es
[b] School of Chemistry, University of Birmingham, Birmingham B15 2TT, U.K.
e-mail: f.fernandez-trillo@bham.ac.uk

† Footnotes relating to the title and/or authors should appear here.
Electronic Supplementary Information (ESI) available: [details of any supplementary information available should be included here]. See DOI: 10.1039/x0xx00000x

Journal Name

ARTICLE

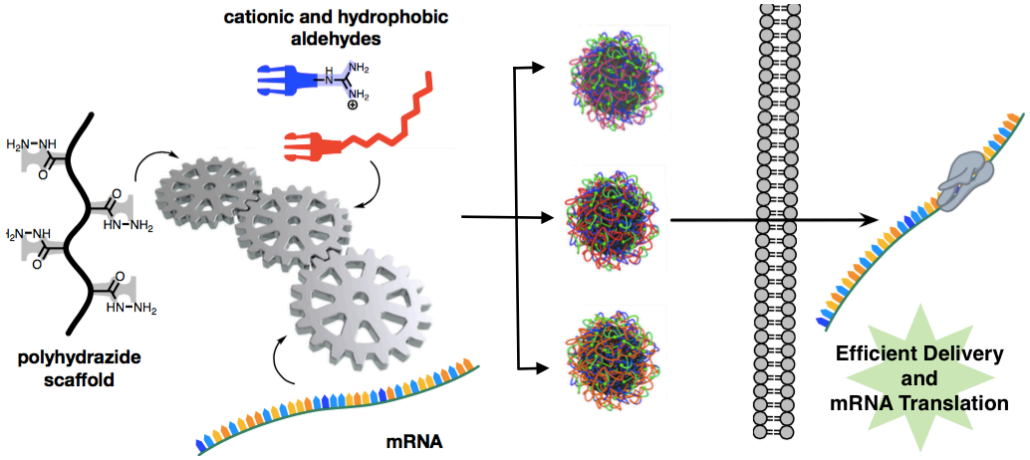

Figure 1. Scheme for the screening of polyhydrazones for mRNA delivery. Polyhydrazides were reacted with a single cationic and different hydrophobic aldehydes. The resulting amphiphilic polymers were incubated with mRNA encoding the green fluorescent protein (EGFP) to obtain different polyplexes employed in transfection experiments.

non-viral vectors, polymers stand out as excellent transfection agents due to their excellent properties and simple synthesis in a range of sizes.[3,43–45] In addition, polymers provide a multivalent scaffold for supramolecular electrostatic/hydrophobic interactions with the nucleic acid cargo, which is key for nucleic acid complexation, cellular recognition[46] and response to external stimuli.[47] As a consequence, polymers are one of the most promising synthetic materials for gene therapy due to their versatility.[3,17,48] Although very interesting recent designs have shown excellent properties,[49,50] the development of new strategies for the simple and costless high-throughput screening technologies for the discovery of mRNA non-viral vectors is strongly beneficial.

We have recently reported the *in situ* conjugation of polyhydrazide scaffolds with cationic and hydrophobic aldehydes to obtain polyhydrazone vectors as an ideal strategy for the identification of new polymeric vectors for small interfering RNA (siRNA) and plasmid DNA in human HeLa cells.[25,26] These polyhydrazides can be functionalized with different aldehydes moieties *in situ*,[51] that is, in aqueous environment and without any isolation or purification steps.[25,26] The resulting amphiphilic polyhydrazones can be then combine with the DNA cargo and screened for the delivery of nucleic acids (i.e. siRNA, pDNA). However, the potential application of these promising polyhydrazones for the delivery of the more challenging mRNA still remained elusive. Prompted by its strong therapeutic possibilities and by the industrial interest in new materials for mRNA delivery, we decided to study the potential of our methodology for the more challenging delivery of the highly sensitive messenger RNA.

Here, we report the application of the *in situ* functionalization of polyhydrazones for the delivery of mRNA to Hek293 cells. Polyhydrazides were modified with a cationic and six different hydrophobic aldehydes to yield amphiphillic polyhydrazones, which were tested for intracellular delivery of mRNA encoding for the synthesis of the enhanced green fluorescent protein (EGFP). In particular, this work confirms that a higher molecular weight of poly(acryloyl hydrazide) and a new hydrophobic aldehydes, none of which were previously reported, are required to achieve efficient mRNA transfection. The results reported here confirmed the potential of these polymers to efficiently complex and deliver mRNA with high efficiency and low cytotoxicity even at low polyhydrazone concentrations.

2. Results and Discussion

2.1 Design and polyhydrazone formation. Following initial transfection experiments that showed that shorter poly(acryloyl hydrazide)s were unable to deliver longer nucleic acids, the synthesis of poly(acryloyl hydrazide) Pn was adapted from our previous work.[25,26,51] In this case, free-radical polymerization using 2-aminoethanethiol as a chain-transfer agent was employed to afford a poly(acryloyl hydrazide) of significantly higher molecular weight that those reported by us so far (See ESI† for full details).[21,22] Following previously reported experimental conditions, polyhydrazide **P** was reacted with a mixture of cationic ($\mathbf{T_1}$) and hydrophobic

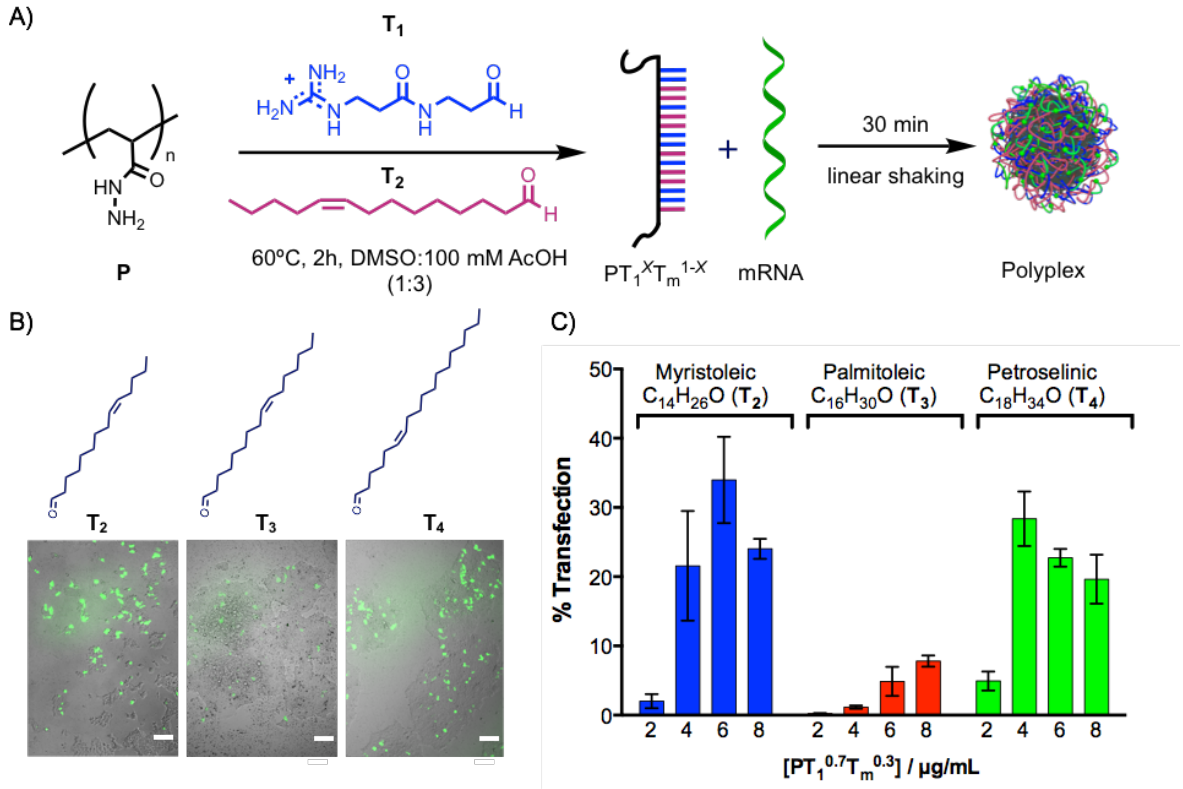

Figure 2. Polyhydrazone reaction and initial screening. (A) Schematic representation of the reaction of the polyhydrazide **P** with the cationic $\mathbf{T_1}$ and the hydrophobic $\mathbf{T_m}$ aldehydes to yield the activated-polyhydrazone that is incubated with the mRNA for transfection experiments. (B) Microscopy images of Hek293 cells incubated with $\mathbf{PT_1^{0.7}/T_m^{0.3}}$. The corresponding hydrophobic aldehydes are indicated above each panel. Scale bars represent 200 nm. (C) Percentage of transfection of **EGFP-mRNA** in Hek293 cells using three different hydrophobic aldehydes. Error bars indicate the standard deviation of three replicates.

aldehydes ($\mathbf{T_m}$) in 100 mM acetate buffer:DMSO (3:1) at 60°C during 2 h.[51] Due to the high Mw of the poly(acryloyl hydrazide) used, a slightly higher proportion of aqueous buffer had to be employed (*i.e.* 3:1 for mRNA delivery as compared to 1:1 for pDNA delivery[26]). After securing complete solubility of all the reagents, the resulting amphiphilic polyhydrazones were directly combined mRNA without further purification (Fig. 2A). As previously reported,[25,26,30] we decided to employ different hydrophobic aldehydes but to keep fixed the cationic guanidinium aldehyde ($\mathbf{T_1}$), because its high pK_a (pK_a~12.5) ensures protonation at physiological pH, which enhances mRNA complexation by electrostatic interactions. The corresponding hydrazone-activated polymers were named $\mathbf{PT_1^{X}T_m^{1-X}}$, where **m** (2-7) is used for the identification of the hydrophobic aldehydes and ***X*** is the molar fraction of the guanidinium aldehyde in the mixture (Fig. 2A).

2.2 mRNA delivery by polyhydrazones. A preliminary mRNA transfection assay was performed in Hek293 cells in order to select combinations of aldehydes for further optimisation (Fig 2B and 2C). Accordingly, polyhydrazide **P** was incubated with guanidinium aldehyde ($\mathbf{T_1}$) and three different hydrophobic aldehydes (myristoleic ($\mathbf{T_2}$), palmitoleic ($\mathbf{T_3}$) and petroselinic ($\mathbf{T_4}$) aldehydes) using the same ratio of hydrophilic to hydrophobic aldehyde that we had previously reported as optimal for the delivery of plasmid DNA ($X\mathrm{T_1}$=0.7, $X\mathrm{T_m}$=0.3).[26] While an excess of aldehyde was used during the post-polymerization modification of poly(acryloyl hydrazide) (7 equiv. per monomer), no transfection is observed with the aldehydes alone.[18,19,25,52] The hydrazone-activated polymers were then incubated with the **EGFP-mRNA** in DMEM medium for 30 min at room temperature (See experimental section for full details) and the resulting polyplexes incubated with Hek293 cells for 5 hours in DMEM. The medium was then replaced by DMEM containing 10% FBS and 1% of Penicillin-Streptomycin-Glutamine Mix, and fluorescence was quantified by flow cytometry 24 hours post-transfection (Fig. 2C). While almost no transfection was observed for the palmitoleic derivative ($\mathbf{T_3}$), both myristoleic ($\mathbf{T_2}$) and petroselinic ($\mathbf{T_4}$) aldehydes showed encouraging values of transfection by epifluorescence microscopy (Fig. 2B). These results were in agreement with the cytometry quantification that indicated a 30% of transfected cells per well for the certain concentrations of the polyhydrazones with the myristoleic ($\mathbf{T_2}$) and the petroselinic ($\mathbf{T_4}$) aldehydes (Fig. 2C).

2.3 Transfection optimization and cell viability. Having confirmed the delivery of mRNA inside Hek293 cells for certain aldehyde combinations, we then performed an optimization of the aldehyde molar fraction for the most promising combination of guanidinium and myristoleic

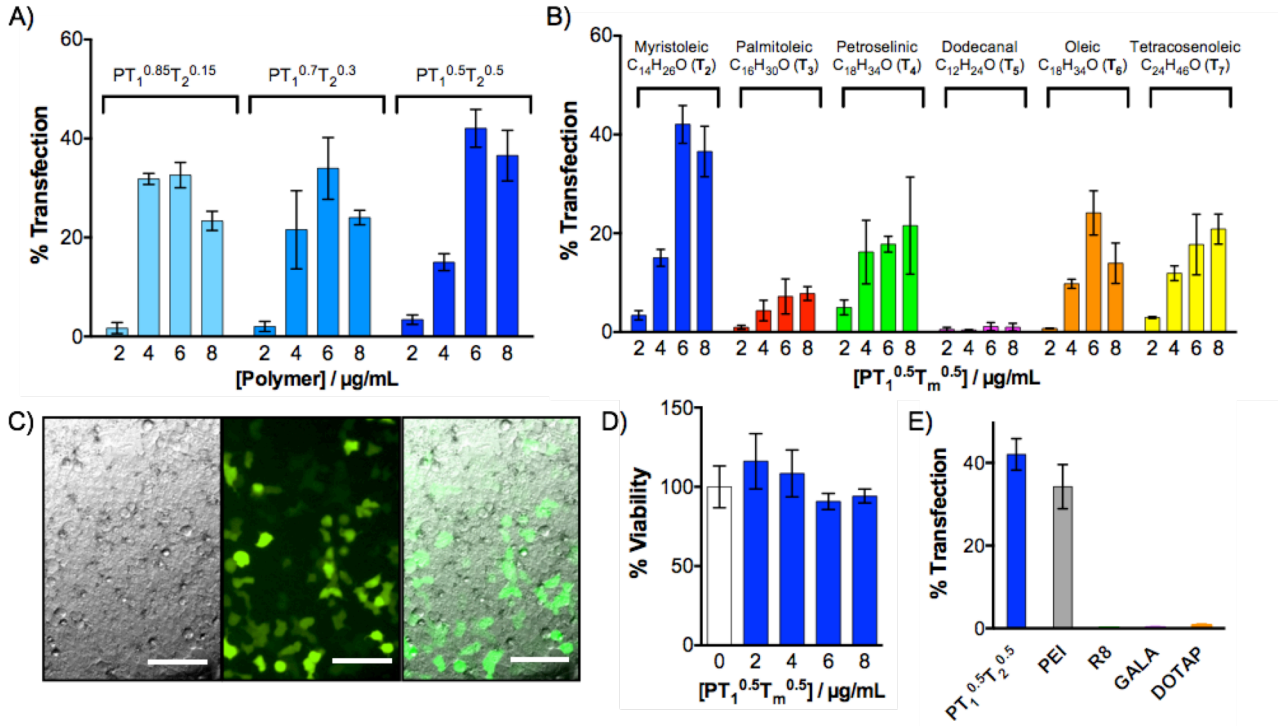

Figure 3. Transfection optimization and cell viability. (A) Molar ratio optimization for the transfection of **EGFP-mRNA** (1 ng/µL) with myristoleic-modified polyhydrazones (**T_2**) at different concentrations. (B) Transfection efficiency of the polymer conjugated with six different hydrophobic aldehydes at different concentrations. **EGFP-mRNA** concentration was kept constant at 1 ng/µL. Data is expressed as the mean of the percentage of transfected cells in three replicates. (C) Bright-field images, green fluorescent channel and merged images of Hek293 cells 24 hours after transfection with polyplexes formed with 6 µg/mL of the myristoleic-modified polymer (*X*$\mathbf{T_1}$:0.5, *X*$\mathbf{T_2}$:0,5) and 1 ng/µL **EGFP-mRNA**. (D) MTT viability assay. Hek293 cells were transfected with the indicated concentrations of the myristoleic-modified polymer and 1 ng/µL of mRNA, and 24 hours after transfection, cell viability was measured with a MTT colorimetric assay. Values were normalized to untreated cells (white bar). E) Transfection efficiency of **EGFP-mRNA** (1 ng/µL) using single component formulations vector/mRNA with vectors: $PT_1^{0.5}T_2^{0.5}$, PEI, R8, GALA and DOTAP), all at 6 µg/mL Scale bars represent 100 nm.

aldehyde (Fig. 3A). These experiments showed slightly higher activities when the molar fraction of the myristoleic aldehyde was increased up to *X*$\mathbf{T_1}$/*X*$\mathbf{T_2}$ = 0.5:0.5. Finally, with this optimized molar ratio ($\mathbf{PT_1^{0.5}/T_m^{0.5}}$), a dose-response transfection experiment was performed using now six hydrophobic aldehydes. Quantification of transfection using flow cytometry showed that all the polyhydrazones investigated, with the exception of the polyhydrazone bearing the dodecanal hydrophobic aldehyde, were capable of transfecting mRNA inside Hek293 cells with good efficiencies (Fig 3B). Once again, the myristoleic aldehyde displayed the highest transfection value (42% of transfected cells per well), suggesting that myristoleic aldehyde outcompetes the rest of the hydrophobic aldehydes in terms of transfection activity. Fluorescence microscopy images of transfected cells visually confirmed the high efficiency of myristoleic-modified polyhydrazones as gene vectors (Fig. 3C). In order to compare the efficiency of the activated polyhydrazone $\mathbf{PT_1^{0.5}/T_2^{0.5}}$ with single component formulations for mRNA cell delivery, we decided to test several cationic and amphiphilic delivery vehicles such as the olicationic penetrating peptide (R8), the pore forming peptide (GALA), the cationic lipid (DOTAP) and the polyethylenimine polymer (PEI). At an equal low weight concentration (6 µgr/ml) of each transfecting reagent, only the cationic polymer (PEI) achieved a similar, slightly lower, level of transfection efficiency compared to that of the activated polyhydrazone $\mathbf{PT_1^{0.5}/T_2^{0.5}}$ (Fig 3E). The lack of transfection of mRNA using penetrating peptides vehicles and cationic liposomes, at low vector concentration, confirmed the suitability of activated polyhydrazones to discover and optimize polymeric formulations for the delivery of the challenging mRNA.

Next, we evaluated the toxicity of the polyhydrazones at the working conditions of the transfection experiments (Fig. 3D and S1). To this end, we employed a colorimetric assay that quantifies cell viability by measuring mitochondrial activity upon reduction of the MTT substrate to purple formazan. To our delight, none of the polyhydrazones investigated showed significant toxicity (Fig S1), in particular those derived from myristoleic aldehyde (Fig. 3D), confirming the excellent properties of these vectors for mRNA delivery.

2.4 Polyplex characterization. To further characterize the polyplexes formed, complexation of mRNA was monitored *via* gel electrophoresis, which confirmed that all polyhydrazones except those derived from dodecanal were

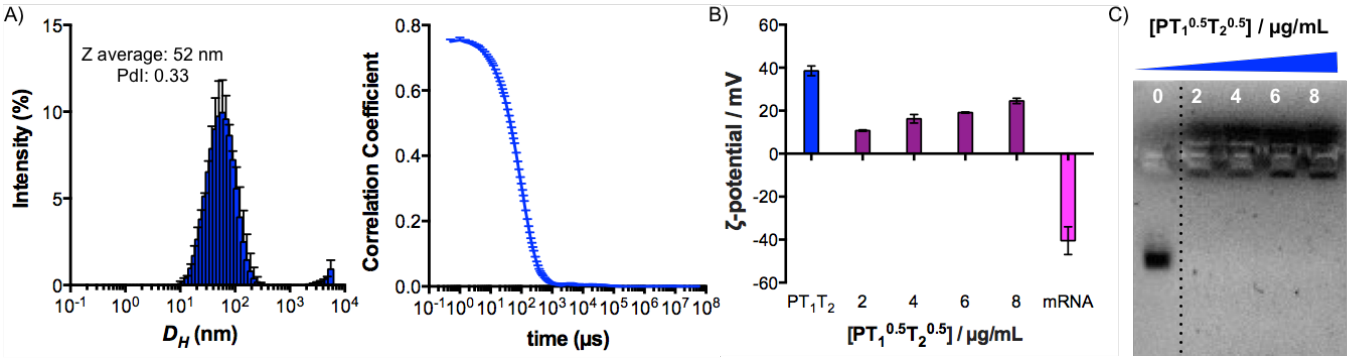

Figure 4. DLS, ζ-potential and gel retardation assay. (A) DLS intensity and correlation curve of myristoleic-modified polymer/**EGFP-mRNA** polyplexes at 6 µg/mL of polyhydrazone, measured in water. (B) Zeta potential (ζ) in millivolts (mV) of myristoleic-modified polymer/EGFP-mRNA polyplexes at 2, 4, 6 and 8 µg/mL of polyhydrazone, measured in water. Data is expressed as mean of triplicates; error bars indicate standard deviation. (C) Gel retardation assay with the myristoleic-modified polyhydrazone. **EGFP-mRNA** and **PT_1T_2/EGFPmRNA** polyplexes with different concentrations of polyhydrazones: 2, 4, 6 and 8 µg/mL. For all experiments [**EGFPmRNA**] = 1 ng/µL.

able to complex mRNA (Fig. 4C and S2). These results were in agreement with those obtained during the transfection experiments, where no activity was found for this particular aldehyde (Fig. 3B), suggesting that saturated aldehydes may not be as active for this application. DLS and Zeta potential measurements were performed for the myristoleic aldehyde polyhydrazones hits (**$PT_1^{0.5}T_2^{0.5}$**, Fig. 4A and 4B). DLS analysis proved the formation of polyplexes with diameters of 50 to 100 nm, with characteristic polyplex PdIs (~0.3),[53] and showed the progressive increase in zeta potential with increasing polymer concentration (Fig. 4B). These results are in agreement with the gel experiments, where the polyhydrazone was able to provide polyplexes with a positive net charge of around 15 mV, enough to inhibit mRNA migration in the gel at all the tested concentrations (Fig. 4C).

3. Conclusions

The objective of this study was to demonstrate the versatility of the in situ polyhydrazone formation as an excellent methodology for the identification of amphiphilic polymers to complex and deliver inside cells the challenging messenger RNA. In this work, a high molecular weight poly(acryloyl hydrazide) was easily functionalized with a mixture of guanidinium and hydrophobic aldehydes. The resulting polyhydrazones were optimized with different hydrophobic aldehydes at different molar ratios to achieve efficient non-viral vehicles for mRNA delivery inside human cells (Hek293) with low toxicity. Our results indicate that amphiphilic polyhydrazones derived from unsaturated aldehydes displayed very good promising transfection capacity of the challenging mRNA, a nucleic acid with a great potential in genetic engineering and gene therapy.

4. Experimental Section

4.1 Materials. Poly(acryloyl hydrazide) was synthesized using controlled free radical polymerization (See ESI† for full details). The aldehydes tested were either commercially available or synthesized following reported protocols from the corresponding alcohols.[52] R8 and GALA were prepared using solid phase peptide synthesis. PEI (linear, MW: 25000) was purchased from Alfa Aesar. DOTAP was acquired from Avanti Polar Lipids. Penicillin-Streptomycin-Glutamine Mix, Trypsin-EDTA solution and DMEM (4500 mg/mL glucose, L-glutamine, sodium pyruvate and sodium bicarbonate) were purchased from Fisher Scientific. Fetal bovine serum was purchased from Sigma-Aldrich. The selected cargo (**EGFP-mRNA**) was a single-stranded EGFP encoding messenger RNA of 996 nucleotides, it is capped and polyadenylated and modified with 5-methoxyuridine. This mRNA was purchased to TriLink Biotechnologies.

4.2 Conjugation of poly(acryoyl hydrazide) with aldehyde modulators. In a typical experiment, poly(acryoyl hydrazide) in acetate buffer (100 mM, pH = 0.3) was reacted with 7 equiv. per monomer of different molar fractions of guanidiniun (**T_1**) and a variety of six hydrophobic (**T_2**) aldehyde tails. For most experiments, 10 µL of a solution of poly(acryoyl hydrazide) (2 mg/mL), 5 µL of a solution of **T_1** (223 mM) both in acetate buffer (100 mM, pH = 3.0) and 5 µL of a solution of **T_2** (223 mM) in dry DMSO were mixed to give a final monomer concentration of 1 mg/mL with a molar ratio X**T_1**=0.5 and X**T_2**=0.5. This mixture was shaken at 60°C for 2 hours. The polyhydrazones obtained were used for Hek293 cells transfection experiments without further purification.

4.3 EGFP-mRNA delivery. Human embryonic kidney 293 cells (Hek293) were maintained in Dulbecco's Modified Eagle's Medium supplemented with 10% FBS and 1% Penicillin-Streptomycin-Glutamine Mix at 37°C/5% CO_2/95% humidity in an INCO 108 incubator (Memmert).

One day before transfection, cells were seeded in 96-well plates at a concentration of 150000 cells/mL (100 µL/well). Transfection was done by incubation of cells with 1 ng/µL of **EGFP-mRNA** and different concentrations of the activated polymers (2-8 µg/mL), previously prepared as

described above. The solutions of polymer/**EGFP-mRNA** were prepared before to the transfection experiments by mixing 10 µL of the **EGFP-mRNA** solution (20 ng/µL in DMEM) and 35 µL of the polymer solution in DMEM for 30 min using linear shaking. Then, 11 µL of every polymer/mRNA mixture was added to Hek293 cells previously covered with 39 µL of DMEM without FBS or antibiotics. Cells were incubated for 5 h prior to exchange the medium for DMEM (without phenol red) containing 10% bovine foetal serum and 1% of Penicillin-Streptomycin-Glutamine Mix.

4.4 Epifluorescence microscopy of transfected cells. Hek293 cells were transfected following the protocol described above. After 24 hours of incubation cells were imaged under the microscope (Fig. 2B and 3C).

4.5 Flow Cytometry. Hek293 cells were transfected following the procedure described above. One day after transfection, cells were trypsinized with 100 µL of Trypsin-EDTA for 10 min at 37°C. After neutralizing trypsin by the addition of 100 µL of 2 % FBS and 5 mM EDTA in PBS, cell clumps were broken by pipetting before analysing on a Guava EasyCyteTM cytometer. EGFP fluorescence was measured by excitation at 488 nm and detection at 512/18 nm. For the analysis, cells with typical FSC and SSC parameters were selected and cells were considered EGFP positive when fluorescence signal was higher than that of the untreated cells (Fig. 2C, 3A and 3B). Data analysis was performed with InCyte software included in GuavaSoft 3.2 (Millipore).

4.6 Cell viability assay. Cell viability was determined using a MTT assay, which relies on the ability of cells to reduce the water-soluble tetrazolium salt to the insoluble formazan. Hek293 cells, seeded at a concentration of 200000 cells/mL the day before to transfection, were incubated with the polyplexes as previously described before performing the assay. After 24 hours of incubation 10 µL of MTT (5 mg/mL stock solution in PBS) were added to the cells and further incubated for 4 hours at 37°C. After incubation, 100 µL of acidified isopropanol (10 % Triton X-100, 0.1 M HCl) were added to the cells for dissolving the formazan crystals. Absorbance was measured at 570 nm using a microplate reader (Infinite F200pro, Tecan). Data points were collected in triplicate and values were normalized for untreated control cells (Fig 3D and S1).

4.7 Hydrodinamic Radius and ζ-Potential. For gel retardation assay, 35 µL of different concentrations of the freshly prepared polyhydrazones (2-8 µg/mL in H_2O) were mixed with 10 µL of **EGFP-mRNA** solution (20 ng/µL in H_2O) and incubated for 30 min with linear shaking. Before measuring, 955 µL of filtered H_2O were added to each solution and size and ζ-potential were resolved in a Malvern Zetasizer NanoZSP using standard disposable cuvettes. All experiments were done in triplicate at 25°C (Fig. 4A and 4B).

4.8 Gel retardation assay. For gel retardation assay, different concentrations of the freshly prepared polyhydrazones were mixed with the **EGFP-mRNA** in DMEM at room temperature for 30 min. The polyplexes and a solution of the free **EGFP-mRNA** at the same concentration were loaded in a 1% agarose gel containing 0.5 µg/mL of ethidium bromide in TAE buffer (40 mM Tris, 20 mM acetic acid and 1 mM EDTA). Electrophoresis was run at 100V for 15 min and gel was imaged under UV light using GelDoc system (Fig. 4C and S2).

Conflicts of interest

In accordance with our policy on Conflicts of interest please ensure that a conflicts of interest statement is included in your manuscript here. Please note that this statement is required for all submitted manuscripts. If no conflicts exist, please state that "There are no conflicts to declare".

Acknowledgements

This work has received financial support from Spanish Agencia Estatal de Investigación (AEI) [CTQ2014-59646-R, SAF2017-89890-R], the Xunta de Galicia (ED431C 2017/25, 2016-AD031 and Centro singular de investigación de Galicia accreditation 2016–2019, ED431G/09) and the European Union (European Regional Development Fund - ERDF). M.J. received a F.P.I. fellowship from MINECO (CTQ2014-59646-R). J.M. received a Ramón y Cajal (RYC-2013-13784), an ERC Starting Investigator Grant (DYNAP- 677786) and a Young Investigator Grant from the Human Frontier Science Research Program (RGY0066/2017). F.F.T. thanks the Birmingham Science City and the European Regional Development Fund, and the University of Birmingham (John Evans Fellowship). O.C. thanks the Midlands Integrative Biosciences Training Partnership (MIBTP) for the PhD scholarship.

Notes and references

1 L. Naldini, *Nature*, 2015, **526**, 351–360.
2 C. E. Dunbar, K. A. High, J. K. Joung, D. B. Kohn, K. Ozawa and M. Sadelain, *Science*, 2018, **359**, eaan4672.
3 I. Lostalé-Seijo and J. Montenegro, *Nat. Rev. Chem.*, 2018, **2**, 258–277.
4 R. S. Riley, C. H. June, R. Langer and M. J. Mitchell, *Nat. Rev. Drug Discov.*, , DOI:10.1038/s41573-018-0006-z.
5 U. Sahin, K. Karikó and Ö. Türeci, *Nat. Rev. Drug Discov.*, 2014, **13**, 759–780.
6 K. J. Kauffman, M. J. Webber and D. G. Anderson, *J. Control. Release*, 2016, **240**, 227–234.
7 N. Pardi, M. J. Hogan, F. W. Porter and D. Weissman, *Nat. Rev. Drug Discov.*, 2018, **17**, 261–279.
8 I. Casanova-Salas, E. Masiá, A. Armiñán, A. Calatrava, C. Mancarella, J. Rubio-Briones, K. Scotlandi, M. J. Vicent and J. A. López-Guerrero, *PLoS One*, 2015, **10**, e0125576.
9 G. Tiram, E. Segal, A. Krivitsky, R. Shreberk-Hassidim, S.

Ferber, P. Ofek, T. Udagawa, L. Edry, N. Shomron, M. Roniger, B. Kerem, Y. Shaked, S. Aviel-Ronen, I. Barshack, M. Calderón, R. Haag and R. Satchi-Fainaro, *ACS Nano*, 2016, **10**, 2028–2045.

10 P. H. Johnson, *ChemMedChem*, 2011, **6**, 1311–1312.

11 O. Vázquez and O. Seitz, *Chem. Sci.*, 2014, **5**, 2850–2854.

12 W. V Gilbert, T. A. Bell and C. Schaening, *Science*, 2016, **352**, 1408–1412.

13 F. Pastor, P. Berraondo, I. Etxeberria, J. Frederick, U. Sahin, E. Gilboa and I. Melero, *Nat. Rev. Drug Discov.*, 2018, **17**, 751–767.

14 N. Pardi and D. Weissman, *Methods Mol. Biol.*, 2017, **1499**, 109–121.

15 Z. Meng, J. O'Keeffe-Ahern, J. Lyu, L. Pierucci, D. Zhou and W. Wang, *Biomater. Sci.*, 2017, **5**, 2381–2392.

16 A. Yamamoto, M. Kormann, J. Rosenecker and C. Rudolph, *Eur. J. Pharm. Biopharm.*, 2009, **71**, 484–489.

17 J. R. D. and D. G. A. Hao Yin, Rosemary L. Kanasty, Ahmed A. Eltoukhy, Arturo J. Vegas, *Nat. Rev. Genet.*, 2014, **15**, 541–555.

18 I. Louzao, R. García-Fandiño and J. Montenegro, *J. Mater. Chem. B*, 2017, **5**, 4426–4434.

19 I. Lostalé-Seijo, I. Louzao, M. Juanes and J. Montenegro, *Chem. Sci.*, 2017, **8**, 7923–7931.

20 X.-L. Zhao, B.-C. Chen, J.-C. Han, L. Wei and X.-B. Pan, *Sci. Rep.*, 2015, **5**, 17640.

21 T. Lehto, K. Ezzat, M. J. A. Wood and S. EL Andaloussi, *Adv. Drug Deliv. Rev.*, 2016, **106**, 172–182.

22 S. Sabnis, E. S. Kumarasinghe, T. Salerno, C. Mihai, T. Ketova, J. J. Senn, A. Lynn, A. Bulychev, I. McFadyen, J. Chan, Ö. Almarsson, M. G. Stanton and K. E. Benenato, *Mol. Ther.*, 2018, **26**, 1509–1519.

23 M. B. De Jesus and I. S. Zuhorn, *J. Control. Release*, 2015, **201**, 1–13.

24 W. Li and F. C. Szoka, *Pharm. Res.*, 2007, **24**, 438–449.

25 J. M. Priegue, D. N. Crisan, J. Martínez-Costas, J. R. Granja, F. Fernandez-Trillo and J. Montenegro, *Angew. Chemie Int. Ed.*, 2016, **55**, 7492–7495.

26 J. M. Priegue, I. Lostalé-Seijo, D. Crisan, J. R. Granja, F. Fernández-Trillo and J. Montenegro, *Biomacromolecules*, 2018, **19**, 2638–2649.

27 A. K. Patel, J. C. Kaczmarek, S. Bose, K. J. Kauffman, F. Mir, M. W. Heartlein, F. Derosa, R. Langer and D. G. Anderson, *Adv. Mater.*, 2019, **1805116**, 1–7.

28 C. J. McKinlay, N. L. Benner, O. A. Haabeth, R. M. Waymouth and P. A. Wender, *Proc. Natl. Acad. Sci.*, 2018, **115**, E5859–E5866.

29 D. Adams, A. Gonzalez-Duarte, W. D. O'Riordan, C.-C. Yang, M. Ueda, A. V. Kristen, I. Tournev, H. H. Schmidt, T. Coelho, J. L. Berk, K.-P. Lin, G. Vita, S. Attarian, V. Planté-Bordeneuve, M. M. Mezei, J. M. Campistol, J. Buades, T. H. Brannagan, B. J. Kim, J. Oh, Y. Parman, Y. Sekijima, P. N. Hawkins, S. D. Solomon, M. Polydefkis, P. J. Dyck, P. J. Gandhi, S. Goyal, J. Chen, A. L. Strahs, S. V. Nochur, M. T. Sweetser, P. P. Garg, A. K. Vaishnaw, J. A. Gollob and O. B. Suhr, *N. Engl. J. Med.*, 2018, **379**, 11–21.

30 G. Gasparini, E. K. Bang, J. Montenegro and S. Matile, *Chem. Commun.*, 2015, **51**, 10389–10402.

31 P. Parvizi-Bahktar, J. Mendez-Campos, L. Raju, N. A. Khalique, E. Jubeli, H. Larsen, D. Nicholson, M. D. Pungente and T. M. Fyles, *Org. Biomol. Chem.*, 2016, **14**, 3080–3090.

32 J. E. Zuckerman and M. E. Davis, *Nat. Rev. Drug Discov.*, 2015, **14**, 843–856.

33 I. Nierengarten, M. Nothisen, D. Sigwalt, T. Biellmann, M. Holler, J. S. Remy and J. F. Nierengarten, *Chem. - A Eur. J.*, 2013, **19**, 17552–17558.

34 T. G. W. Edwardson, T. Mori and D. Hilvert, *J. Am. Chem. Soc.*, 2018, **140**, 10439–10442.

35 J. D. Brodin, A. J. Sprangers, J. R. McMillan and C. A. Mirkin, *J. Am. Chem. Soc.*, 2015, **137**, 14838–14841.

36 P. Boisguérin, S. Deshayes, M. J. Gait, L. O'Donovan, C. Godfrey, C. A. Betts, M. J. A. Wood and B. Lebleu, *Adv. Drug Deliv. Rev.*, 2015, **87**, 52–67.

37 M. Li, S. Schlesiger, S. K. Knauer and C. Schmuck, *Angew. Chemie - Int. Ed.*, 2015, **54**, 2941–2944.

38 M. Li, M. Ehlers, S. Schlesiger, E. Zellermann, S. K. Knauer and C. Schmuck, *Angew. Chemie - Int. Ed.*, 2016, **55**, 598–601.

39 E. Bartolami, Y. Bessin, N. Bettache, M. Gary-Bobo, M. Garcia, P. Dumy and S. Ulrich, *Org. Biomol. Chem.*, 2015, **13**, 9427–9438.

40 E. Bartolami, C. Bouillon, P. Dumy and S. Ulrich, *Chem. Commun.*, 2016, **52**, 4257–4273.

41 A. Fuertes, M. Juanes, J. R. Granja and J. Montenegro, *Chem. Commun.*, 2017, **53**, 7861–7871.

42 S. Ulrich, *Acc. Chem. Res.*, 2019, 10.1021/acs.accounts.8b00591.

43 S. Vaidyanathan, B. G. Orr and M. M. Banaszak Holl, *Acc. Chem. Res.*, 2016, **49**, 1486–1493.

44 B. M. DeRonde, N. D. Posey, R. Otter, L. M. Caffrey, L. M. Minter and G. N. Tew, *Biomacromolecules*, 2016, **17**, 1969–1977.

45 J. Hao, P. Kos, K. Zhou, J. B. Miller, L. Xue, Y. Yan, H. Xiong, S. Elkassih and D. J. Siegwart, *J. Am. Chem. Soc.*, 2015, **137**, 9206–9209.

46 T. T. Smith, S. B. Stephan, H. F. Moffett, L. E. McKnight, W. Ji, D. Reiman, E. Bonagofski, M. E. Wohlfahrt, S. P. S. Pillai and M. T. Stephan, *Nat. Nanotechnol.*, 2017, **12**, 813–820.

47 S. Liu, D. Zhou, J. Yang, H. Zhou, J. Chen and T. Guo, *J. Am. Chem. Soc.*, 2017, **139**, 5102–5109.

48 C. Englert, J. C. Brendel, T. C. Majdanski, T. Yildirim, S. Schubert, M. Gottschaldt, N. Windhab and U. S. Schubert, *Prog. Polym. Sci.*, 2018, **87**, 107–164.

49 E. Wagner, *Acc. Chem. Res.*, 2012, **45**, 1005–1013.

50 C. Sampaio, S. H. Sindrup, J. W. Stauffer, I. Steigerwald, J. Stewart, J. Tobias, R. Treede, M. Wallace and E. Richard, *Biomaterials*, 2017, **127**, 89–96.

51 D. N. Crisan, O. Creese, R. Ball, J. L. Brioso, B. Martyn, J. Montenegro and F. Fernandez-Trillo, *Polym. Chem.*, 2017, **8**, 4576–4584.

52 C. Gehin, J. Montenegro, E. K. Bang, A. Cajaraville, S. Takayama, H. Hirose, S. Futaki, S. Matile and H. Riezman, *J. Am. Chem. Soc.*, 2013, **135**, 9295–9298.

53 I. Insua, A. Wilkinson and F. Fernandez-Trillo, *Eur. Polym. J.*, 2016, **81**, 198–215.